PERGAMON

International Journal of Multiphase Flow 24 (1998) 867–887

International Journal of Multiphase Flow

Force balance in a turbulent particulate channel flow

Koji Fukagata[a,*], Said Zahrai[b], Fritz H. Bark[a]

[a]*Faxén Laboratory, Royal Institute of Technology, 100 44 Stockholm, Sweden*
[b]*ABB Corporate Research, 721 78 Västerås, Sweden*

Received 25 May 1997; received in revised form 13 March 1998

Abstract

Turbulent flows of 70 μm copper particles and 50 μm glass particles in a channel are considered and investigated by large eddy simulations. Only the influence of the background turbulence on the motion of particles is considered and possible modifications of the structure of turbulence due to motion of particles are not accounted for. Mean velocity profiles and RMS levels are presented and are found to be in good agreement with earlier simulation data in literature. Differences between the statistical behavior of the two particle types are presented and discussed. The statistical correlations are used for a detail study of the interphase forces. The dominant contributions in the streamwise and in the wall-normal directions are pointed out. © 1998 Elsevier Science Ltd. All rights reserved.

Keywords: Two-phase flow; Turbulent particulate flow; Large eddy simulation; Particles; Force balance

1. Introduction

Turbulent particulate flows can often occur in industrial processes as well as in the nature. Turbulent particulate flows, in addition to complex phenomena occurring in turbulence, involve processes such as particle dispersion, deposition and entrainment. Moreover the motion of particles affects the structure of carrier turbulence and influences the force balance in the flow. Understanding and modeling of turbulent particulate flows are highly of interest for designing industrial systems and processes involving such flows.

Due to the underlying non-linear nature of turbulent flows and the fact that a large number of particles are present, an analytical solution to the problem cannot be expected. Instead, as is customary in turbulence research, statistical approaches are relied upon also in the case of

* Corresponding author. Department of Quantum Engineering and Systems Science, University of Tokyo, 7-3-1 Hongo, Bunkyo-ku, Tokyo 113, Japan.

PII: S0301-9322(98)00014-7

particulate turbulent flows. In a statistical presentation of the flow, only averaged quantities, such as mean flow and different correlations are of interest and the dynamics of an ensemble of particles is considered rather than the motion of an individual particle.

Purely statistical models cannot be used for prediction of flow in engineering applications. However, they can be a powerful method for understanding the underlying physical phenomena and can contribute to a more accurate modeling.

Reeks (1991, 1992, 1993), starting from Kraichnan's Lagrangian History Direct Interaction Theory (1965), derived a general Green's function for the phase–space probability density of an ensemble of particles in a turbulent flow. The Lagrangian History (LH) equation is valid even when the time scale of the motion of particle is comparable to that of turbulent fluctuations. In that sense the methodology differs from models based on Fokker–Plank equation, where the background turbulence is treated as a white noise. The equations for a certain moment, e.g. Eulerian momentum for particle, stress components etc., are obtained by integrating the product of the moment and the LH equation over all the velocities. Swailes and Reeks (1994) applied homogeneous version of this model (Reeks, 1991) to a deposition problem. The calculated deposition velocity was in good agreement with the empirical relation when the nondimensionalized Stokes relaxation time, τ_p^+, was larger than 100.

During the recent decades, owing to fast development of the capacity of digital computers and numerical computing techniques, simulations of turbulent flows in a direct manner by direct numerical simulations (DNS) or by a low level of modeling in large eddy simulations (LES) have become possible. The advantage of LES in comparison to DNS is its capability of treating flows at high Reynolds numbers. Turbulent particulate flows have recently been investigated by means of numerical simulations. For an efficient investigation of such flows, usually the so-called Eulerian-Lagrangian simulation methodology is used. In this method, the fluid velocity field is obtained by performing DNS or LES of Eulerian equations of motion, while the trajectories of a number of particles are separately calculated by integrating the governing equation of motion for each individual particle.

Wang and Squires (1996a) made use of LES for investigation of dispersed turbulent flow of particles in a channel. In their simulations, both the influence of the motion of particles on the fluid flow and the particle–particle interactions were neglected. The assumption is of course valid for low volume fractions and low mass flow rates. Although the results were in good agreement with DNS by Rouson and Eaton (1994), some discrepancies with the data from experiments by Kulick et al. (1994) were observed. The discrepancies were specially pronounced in regions very near the walls.

Wang and Squires also studied the particle deposition to the wall using the same methodology (Wang and Squires, 1996b) and showed that this methodology can predict the deposition velocity of the particles, whose Stokes relaxation time, τ_p^+, varies from 2 to 6. Influences of the subgrid model on the motion of particles were also investigated which lead to the conclusion that the subgrid scale velocity for the particles in the above range has negligible effect on the statistical quantities.

With further improvement of computer capacity, in long term, direct numerical simulations of fluid flow can be feasible even for large and complicated geometries. However, at the present time, more efficient tools are needed for prediction of flows in industrial processes. The k–ϵ model for predictions of turbulent flows is one of the models which is widely used in

practical applications, mainly because of its robustness. Further development of one point closures for predicting turbulent particulate flows has without doubt a high impact for prediction of flows in industrial processes.

Chen and Wood (1985) proposed a turbulence closure model for dilute gas–particle flow and carried out k–ϵ simulations for an axisymmetric jet. Since particle with small inertia were considered, the mean particle velocity was assumed to be the same as the fluid velocity. The predicted results were in good agreement with experimental data. Bolio and Sinclair (1995) and Cao and Ahmadi (1995) reported on two-fluid modeling of gas-particle flows. In both contributions, the results from k–ϵ simulation using the proposed models were compared with the experimental data by Tsuji et al. (1984).

The aim of this study is to carry out large eddy simulations with Lagrangian particle tracking and provide various statistics of fluid–particle flows which are necessary for accurate modeling by means of one-point closures. In this paper the focus is made on the force balance of the particles in the Eulerian frame and on the related correlations. The paper is organized in the following way. In Section 2, the methodology is outlined. The statistics of particles are presented in Section 3, where the averaged force balance of particle phase is also presented. The results are summarized in Section 4.

2. Methodology

Turbulent flow of a fluid in a channel, sufficiently large in the spanwise and streamwise directions, is considered. The Reynolds number, based on the channel half width and friction velocity, in the undisturbed fluid flow is assumed to be 180. The computational space has a dimension of $4\pi\delta \times 2\pi \times 2\pi\delta$ in x, y and z directions, see Fig. 1. The computational domain was discretized using 32, 42 and 96 cells in x, y and z-directions, see Table 1. No-slip conditions are applied on the walls while periodic boundary conditions are used in the streamwise and the spanwise directions. The fluid flow is modeled exactly as reported in (Zahrai et al., 1995) where a modified Smagorinsky model was used for accounting for the transport of momentum due to subgrid turbulent fluctuations. Zahrai et al. (1995) showed that the methodology predicted the statistical properties of the turbulent channel flow accurately.

In this study, a one-way interaction between the fluid flow and motion of particles is considered and the influence of the motion of particles on the background turbulence and modifications of the structure of turbulence are not accounted for. Motion of the particles is computed by using the Lagrangian method, namely by integrating the particle equation of motion for each individual particle. The particle equation of motion for a single small sphere in a nonuniform flow can be expressed as, see Maxey and Riley (1983),

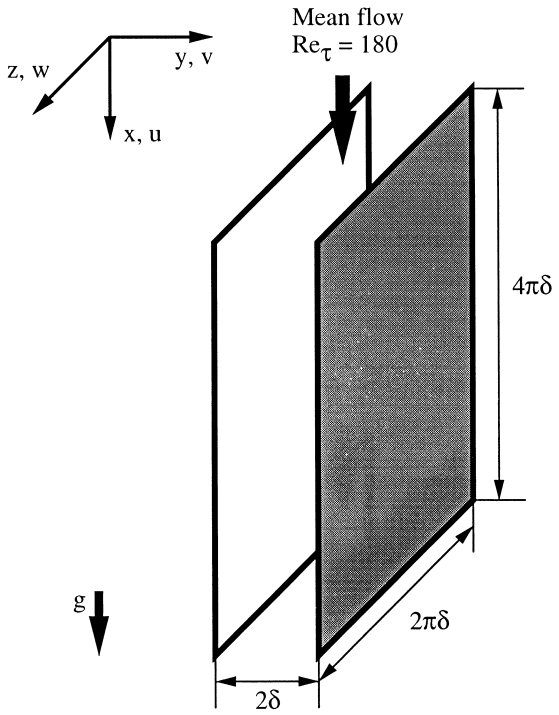

Fig. 1. Geometry of the channel.

$$\begin{aligned}\frac{\mathrm{d}\tilde{u}_i^{\mathrm{p}}}{\mathrm{d}t} &= \frac{18\nu}{d^2 S}\left\{\tilde{u}_i^{\mathrm{f}} - \tilde{u}_i^{\mathrm{p}} + \frac{1}{24}d^2\nabla^2\tilde{u}_i^{\mathrm{f}}\right\} \\ &\quad + \frac{1}{S}\frac{D\tilde{u}_i^{\mathrm{f}}}{Dt} \\ &\quad + \frac{1}{2S}\frac{\mathrm{d}}{\mathrm{d}t}\left\{\tilde{u}_i^{\mathrm{f}} - \tilde{u}_i^{\mathrm{p}} + \frac{1}{40}d^2\nabla^2\tilde{u}_i^{\mathrm{f}}\right\} \\ &\quad + \frac{9\nu}{d^2 S}\int_0^t \mathrm{d}t'\left[\frac{\frac{\mathrm{d}}{\mathrm{d}t'}\left\{u_i^{\mathrm{f}}(t') - u_i^{\mathrm{p}}(t') + \frac{1}{24}d^2\nabla^2 u_i^{\mathrm{f}}(t')\right\}}{\left\{\pi\nu(t-t')\right\}^{1/2}}\right] + \left(1 - \frac{1}{S}\right)g_i, \end{aligned} \tag{1}$$

where $\tilde{u}_i^{\mathrm{p}}$ and $\tilde{u}_i^{\mathrm{f}}$ represent the i-component of instantaneous, particle velocity and local fluid velocity, respectively, and S is the density ratio of particle to fluid, equal to $\rho^{\mathrm{p}}/\rho^{\mathrm{f}}$. Since the particles considered in this study have high density ratio, $S \sim 10^3$, the fluid acceleration term,

Table 1
Mesh specification

N_x	N_y	N_z	Δx^+	Δz^+	$\Delta y^+_{\min}$	$\Delta y^+_{\max}$
32	42	96	70.7	11.8	2.8	18.9

$$\frac{1}{S}\frac{D\tilde{u}_i^{\mathrm{f}}}{Dt},$$

the added mass,

$$\frac{1}{2S}\frac{\mathrm{d}}{\mathrm{d}t}\left\{\tilde{u}_i^{\mathrm{f}}-\tilde{u}_i^{\mathrm{p}}+\frac{1}{40}d^2\nabla^2\tilde{u}_i^{\mathrm{f}}\right\},$$

the history term,

$$\frac{9\nu}{d^2S}\int_0^t \mathrm{d}t'\left[\frac{\mathrm{d}}{\mathrm{d}t'}\left\{u_i^{\mathrm{f}}(t')-u_i^{\mathrm{p}}(t')+\frac{1}{24}d^2\nabla^2u_i^{\mathrm{f}}(t')\right\}/\left\{\pi\nu(t-t')\right\}^{1/2}\right],$$

can be neglected. The particle Reynolds number can be defined as

$$\tilde{R}e_{\mathrm{p}}=\frac{|\tilde{\mathbf{u}}^{\mathrm{f}}-\tilde{\mathbf{u}}^{\mathrm{p}}|d}{\nu}. \tag{2}$$

The Saffman's lift force (Saffman, 1965), is known to overestimate the lift force in cases where the particle Reynolds number is of the order of or larger than unity, see e.g. Mei (1992). Since moderate particle Reynolds numbers are considered here the lift force has been neglected. The Stokes' expression for the drag forces is not valid for moderate particle Reynolds numbers and must be modified due to the flow separation behind the particle. In this study, an empirical drag coefficient (Clift et al., 1978) was adopted. The simplified particle equation will then read

$$\frac{\mathrm{d}\tilde{u}_i^{+p}}{\mathrm{d}t^+}=-\tilde{\beta}^+\left(\tilde{u}_i^{+p}-\tilde{u}_i^{+f}\right)+g_i^+, \tag{3}$$

where the superscript ' + ' denotes variables nondimensionalized by inner scale, e.g.

$$u^+=\frac{u}{u_\tau}, \tag{4}$$

$$x^+=\frac{xu_\tau}{\nu} \tag{5}$$

and

$$t^+=\frac{tu_\tau^2}{\nu}. \tag{6}$$

The channel half width, δ, was assumed to be 9×10^3 m, the friction velocity, u_τ, 0.3 m/s and the kinematic viscosity of the fluid, ν, 1.5×10^{-5} m^2/s, wherever numerical values were needed.

The first term in the right-hand side of the particle equation of motion (3) is the drag force with the drag coefficient β^+ including the empirical correlation defined as

$$\tilde{\beta}^+=\frac{1}{\tau_{\mathrm{p}}^+}\left(1+0.15\tilde{R}e_p^{0.687}\right), \tag{7}$$

Table 2
Specifications of particles

Case	70 μm copper	50 μm glass
d^+	1.42	1.02
S	7184	2040
τ_p^+	810	117
$\tau_p u_\tau/\delta$	4.5	0.65

where τ_p^+ is the Stokes relaxation time of particle with a diameter, d, and a density ratio, S,

$$\tau_p^+ = \frac{18}{d^{+2}S}. \tag{8}$$

The particle equation of motion was numerically integrated using third-order Adams–Bashforth scheme. Both in the calculations of fluid velocity field and the particle trajectories, the discrete time step, Δt, was set to $1 \times 10^{-3}\ \delta/u_\tau$. The fluid velocities, calculated at the locations defined by mesh, were interpolated to the particle locations. Nearest grid point (NGP), linear, and sixth order Lagrangian interpolation schemes were examined. As investigated by Wang and Squires (1996b), the subgrid scale model for particles has negligible effects for the statistics of particles with high inertia, hence neglected in this study. Similarly to the calculation of the fluid velocity field, periodic boundary conditions were applied for the particle passing through the streamwise and the spanwise boundaries. The particles were assumed to bounce elastically on the walls.

3. Results

Simulations were carried out for two different types of particles, copper particles with a diameter of 70 μm and glass particles with a diameter of 50 μm. The 70 μm copper particle had a nondimensional diameter of 1.42 and density ratio of 7184, giving a nondimensionalized Stokes relaxation time of $\tau_p^+ = 810$. The nondimensionalized diameter and the density ratio of the 50 μm glass particle was 1.02 and 2040, respectively, which resulted in a Stokes relaxation time of $\tau_p^+ = 117$ (see Table 2). At the beginning of simulations, $t = 0$, 250 000 particles were distributed homogeneously in the turbulent channel flow. The sample size was chosen exactly same as LES by Wang and Squires (1996a) and the previous study by the authors (Fukagata et al., 1997). Initially, the particle velocities were set to the same values as the local fluid velocities. The equations of motion had been integrated during an initial period of time, the development time, before the statistics were accumulated in order to allow the statistical quantities to become independent of the initial condition.

Fig. 2 shows the time-development of the number of 70 μm copper particles hitting the wall and the momentum change due to particle-wall collisions per unit time. The linear interpolation was used here. The quantities presented in Fig. 2 are values averaged over 100 steps, i.e. 0.1 δ/u_τ. According to this figure, the number of particles hitting the wall seems to become constant, about 6000 particles per unit time, after 6 δ/u_τ. A longer integration time,

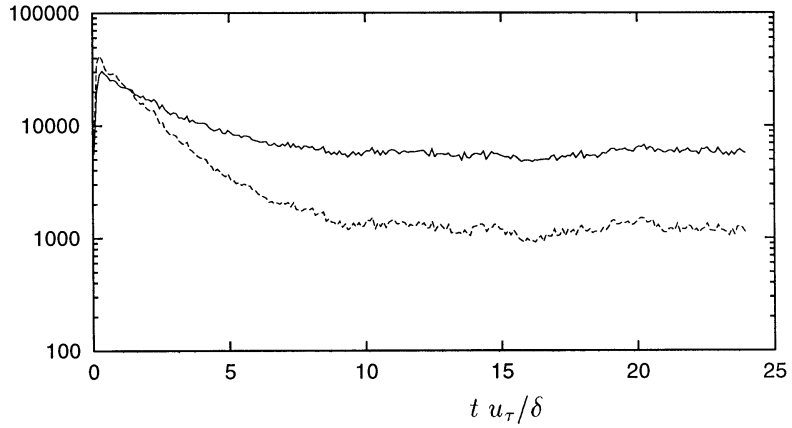

Fig. 2. Time-development of the number of particles hitting the wall and the momentum gained from the wall per unit time. 70 μm copper particles. —, number of particle hitting the wall. - - - -, momentum change due to bouncing at the wall, $\Sigma 2\tilde{v}_{\mathrm{p}}^{+}$.

approximately 10 δ/u_τ, is required for the momentum change to relax to its steady value of 120 u_τ. In this study, two different statistics accumulation periods were used for 70 μm particles. One is after the number of particles hitting the wall has reached equilibrium, $6 < t\ u_\tau/\delta < 12$, and the other is after the momentum change at the wall has converged, $12 < t\ u_\tau/\delta < 24$. The statistics accumulated during $6 < t\ u_\tau/\delta < 12$ were compared with the earlier work by Wang and Squires (1996a) who used the same accumulation period of time. For 50 μm glass particles, two different accumulation periods, $2.4 < t\ u_\tau/\delta < 8.4$ and $8.4 < t\ u_\tau/\delta < 18.4$ were chosen similarly as the previous case.

The statistical values were either averaged on the particle locations, denoted by $\langle\cdot\rangle^{\mathrm{p}}$ or in the whole control volume, denoted by $\langle\cdot\rangle^{\mathrm{f}}$. According to Monin and Yaglom (1971), an averaging operation concerning a certain function, $\tilde{f}(\tilde{u}_i)$, can be defined as

$$<\tilde{f}>=\int_{-\infty}^{\infty}\int_{-\infty}^{\infty}\int_{-\infty}^{\infty}\tilde{f}(\tilde{u}_i)\,P(\tilde{u}_i)\,d\tilde{u}_i, \tag{9}$$

where $P(\tilde{u}_i)$ represents the probability density function of $\tilde{u}_i$ ($i = 1,2,\ldots$). In a channel flow, the statistical quantities are assumed to be a function of only the distance to the walls, y according to Fig. 1. In this study, for a spatially discretized function, its average over particle locations at a distance corresponding to a mesh plane centered at $(\cdot, M_y,\cdot)$ was defined as

$$F^{\mathrm{p}}|_{M_y}=<\tilde{f}>^{\mathrm{p}}|_{M_y}=\frac{1}{N|_{M_y}}\sum_{k=1}^{N|_{M_y}}\tilde{f}\left(\tilde{u}_i^{(k)}\right), \tag{10}$$

where $N|_{M_y}$ denotes the number of samples in the plane centered at $(\cdot, M_y,\cdot)$ during the accumulation period of statistics, and $\tilde{u}^{(k)}{}_i$ denotes the value of $\tilde{u}_i$ at the kth sample. Similarly, the average based on whole control volume can be computed as

$$F^{\mathrm{f}}|_{M_y} = <\tilde{f}>^{\mathrm{f}}|_{M_y} = \frac{1}{N_t N_x N_z}\sum_{I_t=0}^{N_t}\sum_{I_x=1}^{N_x}\sum_{I_z=1}^{N_z}\tilde{f}\left(\tilde{u}_i|_{I_x,M_y,I_z}\right), \tag{11}$$

where $\tilde{u}_i|_{I_x}$, M_y, I_z is the value of $\tilde{u}_i$ in the (I_x, M_y, I_z)-th cell, I_t is the time step, N_t is the total number of time steps, and N_i is the total number of control volumes in ith direction.

Fig. 3a–d and 4a–d show the mean velocities of the fluid, $U^{+\mathrm{f}} = <\tilde{u}^{+\mathrm{f}}>^{\mathrm{f}}$ and that of the particles, $U^{+\mathrm{p}} = <\tilde{u}^{+\mathrm{p}}>^{\mathrm{p}}$, the streamwise and wall-normal root-mean-square (RMS) velocities of fluid and particles, i.e. $u^{+\mathrm{f}}_{\mathrm{rms}} = \sqrt{<(\tilde{u}^{+\mathrm{f}} - <\tilde{u}^{+\mathrm{f}}>^{\mathrm{f}})^2>^{\mathrm{f}}}$, and the number density profile of particles nondimensionalized by the initial number density. In those figures, four different statistics, calculated using three different interpolation schemes and accumulated in two different periods, are presented. In all cases, the computed statistics are in good agreement with the earlier study by Wang and Squires (1996a). Although Wang and Squires (1996b) found, using a fully-developed frozen velocity field in a channel and 250 000 particles randomly distributed in the channel, that the linear interpolation cause large errors in RMS fluid velocity fluctuations computed at the particle locations. Fig. 3a–d shows that the error due to the linear

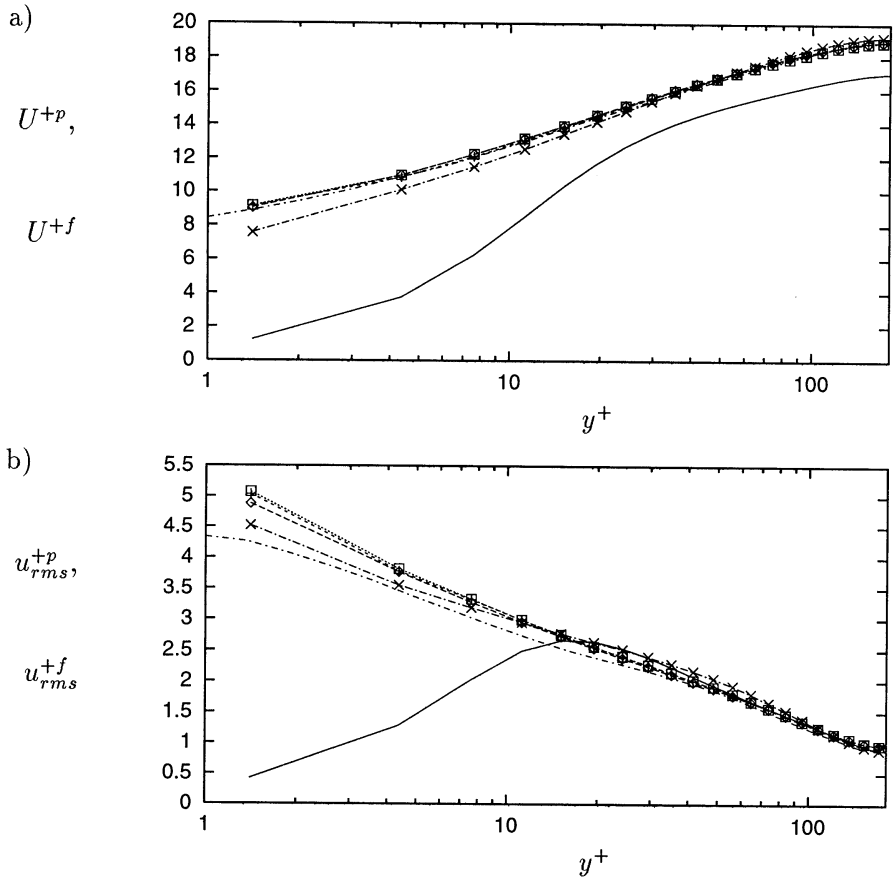

Fig. 3a—*Caption opposite*

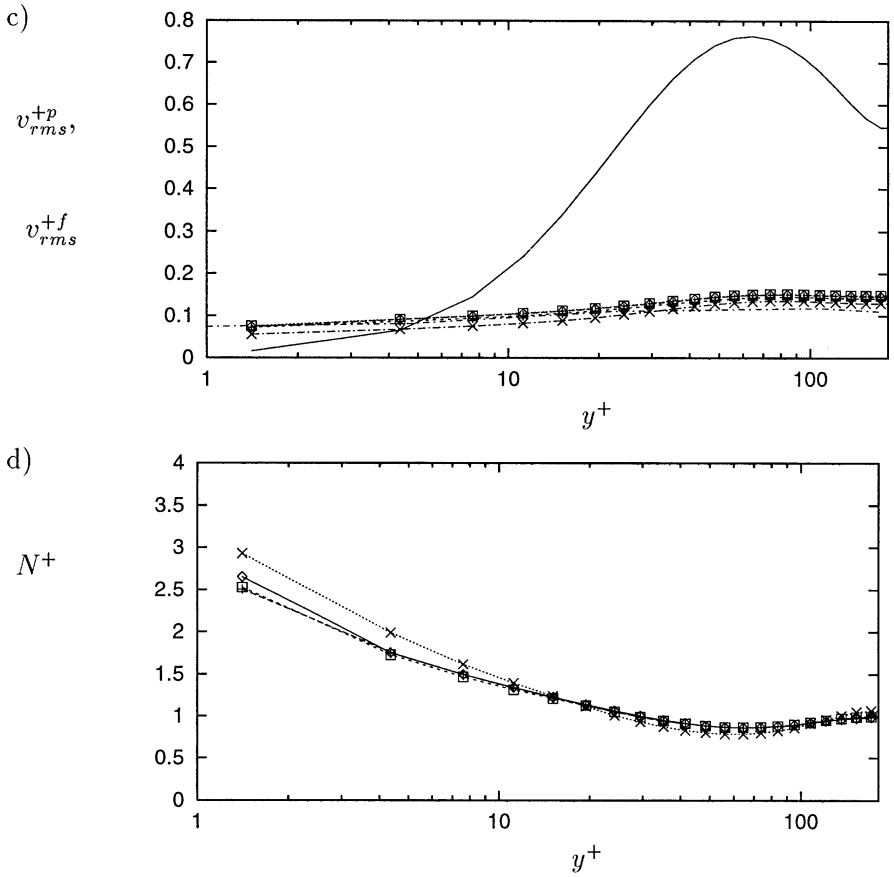

Fig. 3. (a) Mean streamwise velocity; (b) RMS streamwise velocity fluctuation of 70 μm copper particles in a turbulent channel flow at $Re_\tau = 180$. —, fluid. Particle statistics accumulated during $6 < t\,u_\tau/\delta < 12$: -◇-, NGP interpolation; - + -, linear interpolation; - -□- -, sixth order Lagrangian interpolation; - - - -, LES by Wang and Squires (1996a). Particle statistics accumulated during $12 < t\,u_\tau/\delta < 24$: - -x- -, linear interpolation. (c) RMS wall-normal velocity fluctuation; (d) number density profile of 70 μm copper particles in a turbulent channel flow at $Re_\tau = 180$. —, fluid. Particle statistics accumulated during $6 < t\,u_\tau/\delta < 12$: -◇-, NGP interpolation; - + -, linear interpolation; - -□- -, sixth-order Lagrangian interpolation; - - - -, LES by Wang and Squires (1996a). Particle statistics accumulated during $12 < t\,u_\tau/\delta < 24$: - -x- -, linear interpolation.

interpolation does not accumulate. This might be due to the large Stokes relaxation time of particles, which implies that the particles are less sensitive to the small fluctuations in fluid velocity which may be smoothed out by a low-order interpolation scheme. In the same figure, one can notice that two different accumulation periods make slight differences in the statistics very near the wall, however, the differences are negligible in the larger part of channel.

In Fig. 4a–d, the statistics of 50 μm glass particles are presented. Compared to the case of 70 μm copper particles, 50 μm glass particles have a much lower density. The lower density influences both the inertial and gravitational forces resulting in higher RMS levels for wall-normal velocity and smaller differences in the mean velocity. Also these figures show that there are slight differences very near the wall between the statistics from these two accumulation

periods. This ensures that the flows have been fully developed and particle statistics can be used for analysis of various correlation terms appearing in the two-fluid model equations, as will be presented later in the paper.

It was found both in the case of 70 μm copper particles and the case of 50 μm glass particles that the difference in the accumulation periods, i.e. one after the number of particles hitting the wall reached equilibrium and the other after the momentum changes at the wall, do not cause changes in the particle statistics in the larger part of the channel. Differences are observable in the close vicinity of the wall.

To study the detailed differences near the wall, the probability density functions of the streamwise particle velocity were computed. The probability density functions for the 70 μm copper particles at the plane around $y^+ = 6$ and $y^+ = 40$ are depicted in Fig. 5a,b, respectively. Similarly to the experimental observation by Kulick et al. who studied the flow of 70 μm copper particles in a flow at $Re_\tau = 644$, the particle velocity distribution near the wall can be considered bimodal. The high velocity mode, which may be considered as contribution from the particles scarcely interacting with the viscous sublayer, has the maximum point around $u^+ = 15$. The low velocity mode, which may be interpreted as the contribution from

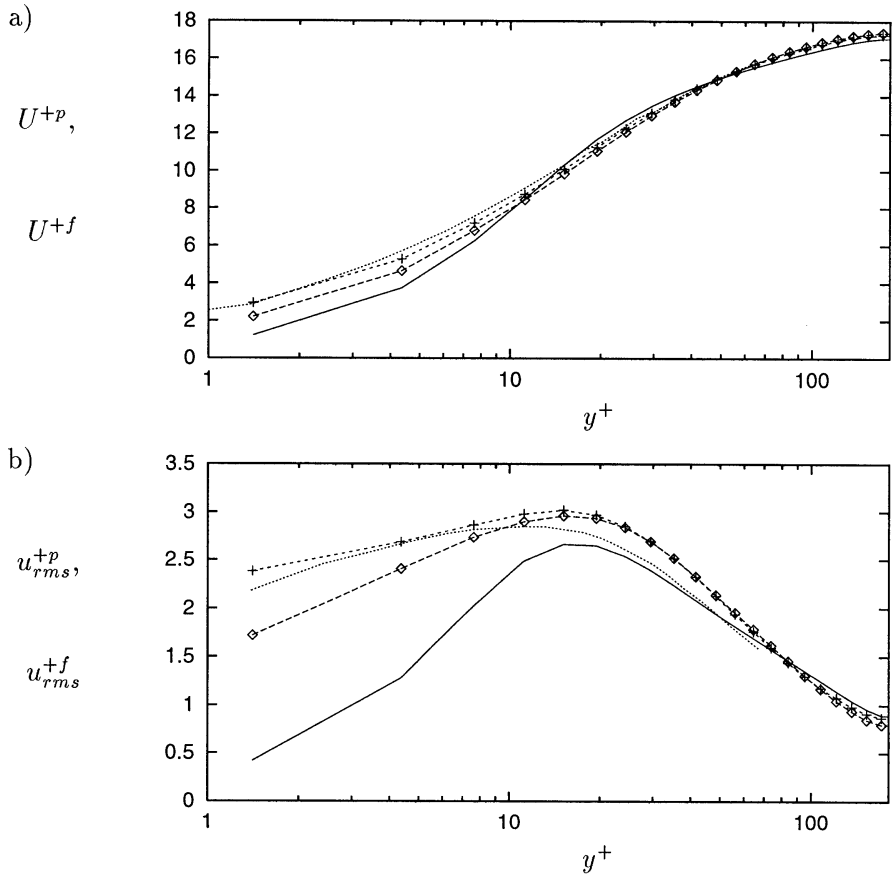

Fig. 4a—*Caption opposite.*

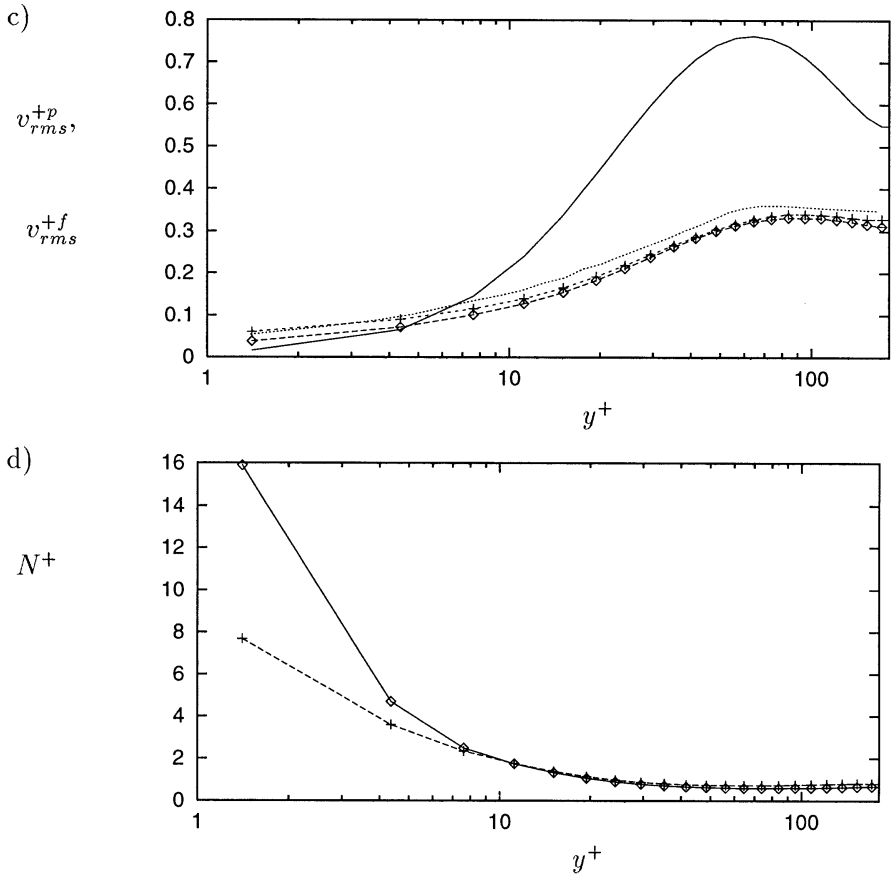

Fig. 4. (a) Mean streamwise velocity; (b) RMS streamwise velocity fluctuation; of 50 μm glass particle in turbulent channel flow at $Re_\tau = 180$. —, fluid; -◇-, particle, accumulated during $8.4 < t\ u_\tau/\delta < 18.4$; - + -, particle, accumulated during $2.4 < t\ u_\tau/\delta < 8.4$; - - -, particle, LES by Wang and Squires (1996a), accumulation period unreported. (c) RMS wall-normal velocity fluctuation; (d) number density profile of 50 μm glass particle in turbulent channel flow at $Re_\tau = 180$. —, fluid; -◇-, particle, accumulated during $8.4 < t\ u_\tau/\delta < 18.4$; - + -, particle, accumulated during $2.4 < t\ u_\tau/\delta < 8.4$; - - -, particle, LES by Wang and Squires (1996a), accumulation period is unreported.

low velocity particles coming from the wall region, has a maximum around $u^+ = 6$. From comparison between the probability functions taken during $12 < t\ u_\tau/\delta < 24$ and those of $6 < t\ u_\tau/\delta < 12$, one finds that the low velocity mode and the high velocity mode have almost the same probability during $6 < t\ u_\tau/\delta < 12$. The low velocity mode became more probable during $12 < t\ u_\tau/\delta < 24$ possibly due to the increase of particle density in the wall region. In the buffer layer, the behavior was found to be somewhat different. The contribution from low velocity particles and high velocity particles increased slightly while the contribution from particles with a streamwise velocity of $14 < \tilde{u}^+ < 18$ decreased.

Similar probability density functions for 50 μm glass particles are shown in Fig. 6a,b. The velocity distribution near the wall is found to be completely different from that of 70 μm copper particles. Only one mode could be found with a maximum at a velocity close to the

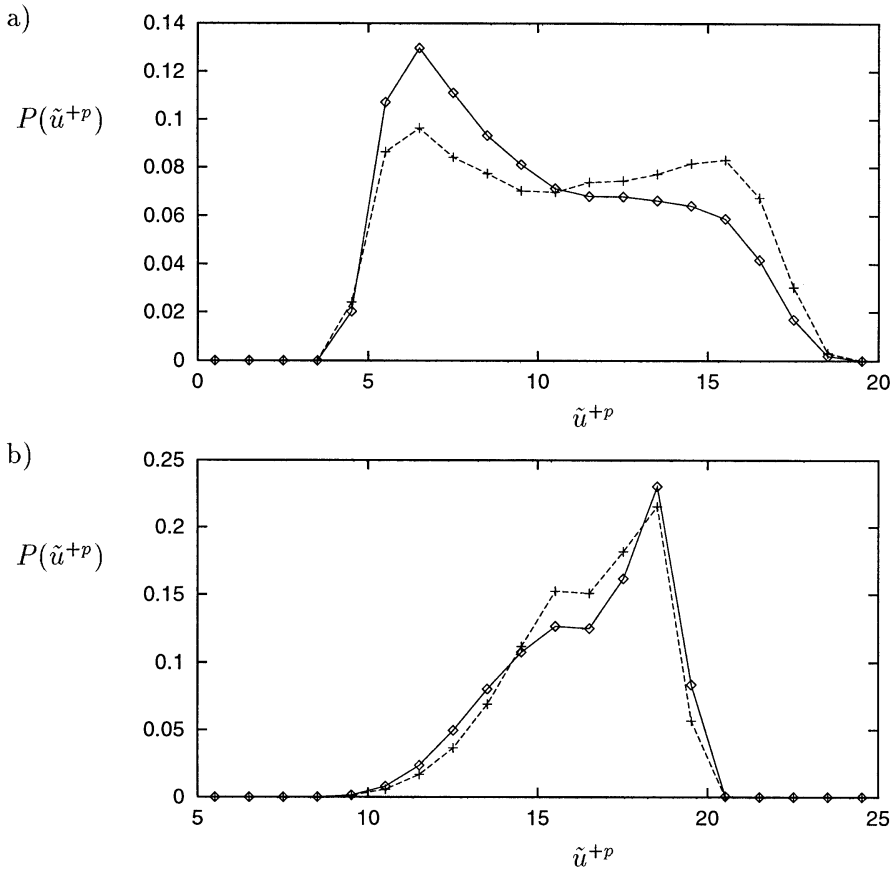

Fig. 5. Probability density function of streamwise particle velocity for 70 μm copper particles: (a) at $y^+ = 6$; (b) at $y^+ = 40$. -◇-, statistics were accumulated during $12 < t\,u_\tau/\delta < 24$; - + -, $6 < tu_\tau/\delta < 12$.

local fluid velocity. The shape of the velocity distribution in the buffer layer is similar to that of 70 μm copper particles with a maximum shifted to lower velocities. The similarities and differences between probability density functions for 70 μm copper particles and 50 μm glass particles at $y^+ > 40$ may suggest a strong dependence of the velocity distribution in the buffer region on the streamwise velocity distribution at in the outer region, $y^+ > 40$.

The statistics of particles were calculated and presented above for a qualitative study of the flow. In what follows, the statistics obtained during the later accumulation periods, i.e. $12 < t\,u_\tau/\delta < 24$ for 70 μm copper particles and $8.4 < t\,u_\tau/\delta < 18.4$ for 50 μm glass particles, in the simulations using the linear interpolation are used for a quantitative investigation of averaged force balance acting on particles in an Eulerian frame.

The Eulerian equations of motion for a particulate turbulent flow can be derived as follows. For a monodispersed particulate flow with a constant particle density, ρ^{p}, which is the case here, the continuity equation for the dispersed phase can be formulated for the instantaneous volume fraction of particle, α^{p}, which can be written as

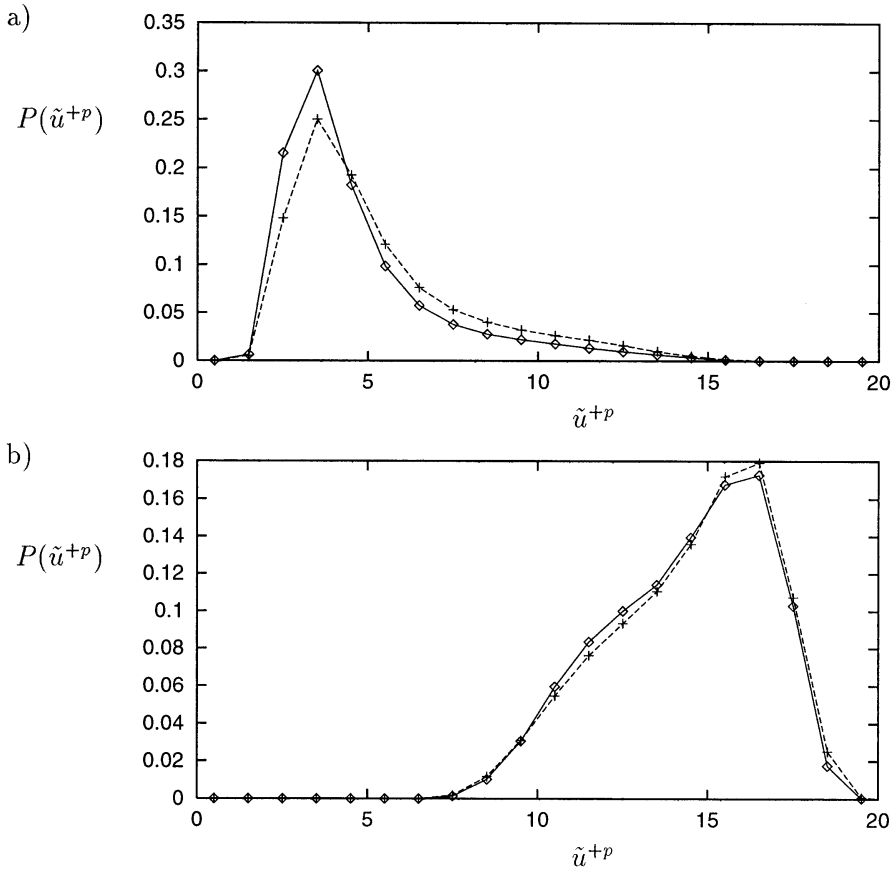

Fig. 6. Probability density function of streamwise particle velocity for 50 μm glass particles. (a) at $y^+ = 6$; (b) at $y^+ = 40$. -◇-, statistics were accumulated during $8.4 < t\,u_\tau/\delta < 18.4$; - + -, $2.4 < tu_\tau/\delta < 8.4$.

$$\rho^{\mathrm{p}} \frac{\partial \tilde{\alpha}^{\mathrm{p}}}{\partial t} + \rho^{\mathrm{p}} \frac{\partial}{\partial x_i}\left(\tilde{\alpha}^{\mathrm{p}}\, \tilde{u}_i^{\mathrm{p}}\right) = 0. \tag{12}$$

The equation of conservation of momentum can similarly be written as

$$\rho^{\mathrm{p}} \frac{\partial \tilde{\alpha}^{\mathrm{p}}\, \tilde{u}_i^{\mathrm{p}}}{\partial t} + \rho^{\mathrm{p}} \tilde{\alpha}^{\mathrm{p}}\, \tilde{u}_j^{\mathrm{p}} \frac{\partial \tilde{u}_i^{\mathrm{p}}}{\partial x_j} = -\tilde{f}_i + \rho^{\mathrm{p}} \tilde{\alpha}^{\mathrm{p}} g_i, \tag{13}$$

where the drag force term, $\tilde{f}_i$, can easily be determined from a comparison with eqn (3) as

$$\tilde{f}_i = \rho^{\mathrm{p}}\, \tilde{\alpha}^{\mathrm{p}} \tilde{\beta}\left(\tilde{u}_i^{\mathrm{p}} - \tilde{u}_i^{\mathrm{f}}\right). \tag{14}$$

In the following, for simplicity, the nondimensional particle number density, $\tilde{n}^+$, defined by

$$\tilde{n}^+ = \frac{\tilde{\alpha}^{\mathrm{p}}}{\alpha^0}, \tag{15}$$

where the constant, α^0, being the global volume fraction, is introduced. The continuity equation and the momentum equation nondimensionalized using viscous scales, the particle density and the global volume fraction then read

$$\frac{\partial \tilde{n}^+}{\partial t^+} + \frac{\partial}{\partial x_i^+}\left(\tilde{n}^+ \tilde{u}_i^{+p}\right) = 0 \tag{16}$$

and

$$\frac{\partial \tilde{n}^+ \tilde{u}_i^{+p}}{\partial t^+} + \tilde{n}^+ \tilde{u}_j^{+p} \frac{\partial \tilde{u}_i^{+p}}{\partial x_j^+} = -\tilde{f}_i^+ + \tilde{n}^+ g_i^+, \tag{17}$$

where

$$\tilde{f}_i^+ = \tilde{n}^+ \tilde{\beta}^+ \left(\tilde{u}_i^{+p} - \tilde{u}_i^{+f}\right). \tag{18}$$

By applying the Reynolds decomposition and by assuming that the flow is homogeneous in the streamwise and the spanwise directions, the momentum equations can be written as

$$\begin{cases} N^+ V^{+\mathrm{p}} \dfrac{\mathrm{d}U^{+p}}{\mathrm{d}y^+} &= -\dfrac{\mathrm{d}}{\mathrm{d}y^+} N^+ < u^{+\mathrm{p}} v^{+\mathrm{p}} >^{\mathrm{p}} - < n^+ v^{+\mathrm{p}} >^{\mathrm{p}} \dfrac{\mathrm{d}U^{+\mathrm{p}}}{\mathrm{d}y^+} \\ & \quad -\dfrac{\mathrm{d}}{\mathrm{d}y^+} V^{+\mathrm{p}} < n^+ u^{+\mathrm{p}} >^{\mathrm{p}} - F_x^+ + N^+ g^+ \\ N^+ V^{+\mathrm{p}} \dfrac{\mathrm{d}V^{+p}}{\mathrm{d}y^+} &= -\dfrac{\mathrm{d}}{\mathrm{d}y^+} N^+ < v^{+\mathrm{p}} v^{+\mathrm{p}} >^{\mathrm{p}} - < n^+ v^{+\mathrm{p}} >^{\mathrm{p}} \dfrac{\mathrm{d}V^{+\mathrm{p}}}{\mathrm{d}y^+} \\ & \quad -\dfrac{\mathrm{d}}{\mathrm{d}y^+} V^{+\mathrm{p}} < n^+ v^{+\mathrm{p}} >^{\mathrm{p}} - F_y^+ \end{cases} \tag{19}$$

In this derivation, the continuity equation was used and the third-order correlation terms including the particle number density fluctuations were neglected similarly to the treatment by Chen and Wood (1985).

The left-hand side of the equation in the y-direction represents the mean convection of the particles. Among others, the first term in the right-hand side is the transport of the momentum of particles by velocity fluctuations, and the last term is the averaged drag force in the wall-normal direction, which can be directly obtained by averaging the drag term in the particle equation of motion, eqn (3).

Different terms involved in the Reynolds averaged equations according to eqn (19) were computed and are presented in Fig. 7. According to that figure, both in the case of 70 μm copper particles and 50 μm glass particles, the averaged drag force in the wall-normal direction, F_y^+, was balanced by the turbulent transport term, $-\mathrm{d}/\mathrm{d}y^+ N^+ < v^{+\mathrm{p}} v^{+\mathrm{p}} >$ and that the other terms seemed to be negligible. According to the data, for example in the case of 70 μm copper particles, the mean convection term, $N^+ V^{+\mathrm{p}} \mathrm{d}V^{+\mathrm{p}}/\mathrm{d}y^+$, was of order of 10^{-7}, and

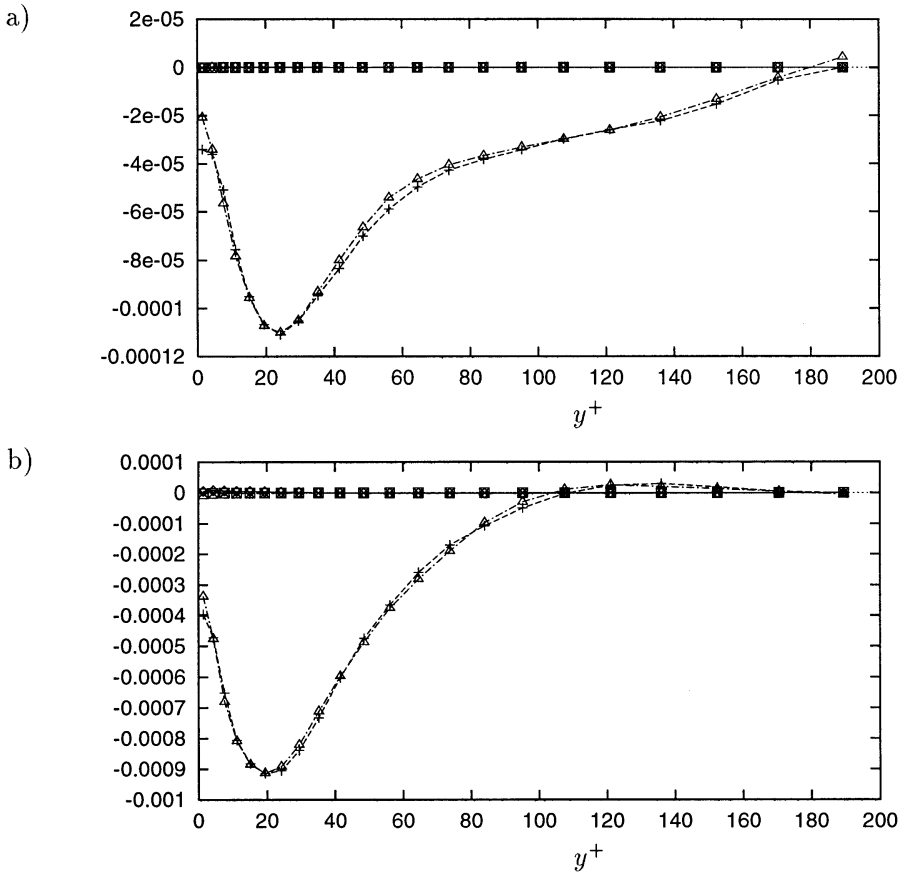

Fig. 7. Different terms in y-direction of particle momentum eqn [19]: (a) 70 μm copper particles; (b) 50 μm glass particles. -◇-,$N^+V^{+\mathrm{p}}\frac{\mathrm{d}V^{+\mathrm{p}}}{\mathrm{d}y^+}$; - + -, $-\frac{\mathrm{d}}{\mathrm{d}y^+}N^+ < v^{+\mathrm{p}}v^{+\mathrm{p}} >^{\mathrm{p}}$; - -□- -, $- < n^+v^{+\mathrm{p}} >^{\mathrm{p}}\frac{\mathrm{d}V^{+\mathrm{p}}}{\mathrm{d}y^+}$; - -x- -, $\frac{\mathrm{d}}{\mathrm{d}y^+}V^{+\mathrm{p}} < n^+v^{+\mathrm{p}} >^{\mathrm{p}}$; - -△- -, F_y^+.

the term, $- < n^+ v^{+\mathrm{p}} >^{\mathrm{p}} \mathrm{d}V^{+\mathrm{p}}/\mathrm{d}y^+$, and the term, $\mathrm{d}/\mathrm{d}y^+ V^{+\mathrm{p}} < n^+ v^{+\mathrm{p}} >^{\mathrm{p}}$, were both of order of 10^{-8} at maximum.

The averaged drag term, F^+_y, can be decomposed to

$$\begin{aligned} F_y^+ &= < \tilde{n}^+\tilde{\beta}^+\left(\tilde{v}^{+\mathrm{p}} - \tilde{v}^{+\mathrm{f}}\right) >^{\mathrm{p}} \\ &= N^+B^+\left(V^{+\mathrm{p}} - V^{+\mathrm{fp}}\right) + N^+ < \beta^+\left(v^{+\mathrm{p}} - v^{+\mathrm{f}}\right) >^{\mathrm{p}} \\ &\quad + B^+ < n^+\left(v^{+\mathrm{p}} - v^{+\mathrm{f}}\right) >^{\mathrm{p}} + \left(V^{+\mathrm{p}} - V^{+\mathrm{fp}}\right) < n^+\beta^+ >^{\mathrm{p}} \\ &\quad + < n^+\beta^+\left(v^{+\mathrm{p}} - v^{+\mathrm{f}}\right) >^{\mathrm{p}} . \end{aligned} \tag{20}$$

In the above formula $V^{+\mathrm{fp}}$ denotes the mean fluid velocity at particle positions, i.e. $V^{+\mathrm{fp}} = < \tilde{v}^{+\mathrm{f}} >^{\mathrm{p}}$. According to the accumulated statistics, see Fig. 8, the main contributions to averaged wall-normal drag force were from the fluctuating force due to the correlation between the fluctuating non-linear drag and the fluctuating velocity, $N^+ < \beta^+(v^{+\mathrm{p}} - v^{+\mathrm{f}}) >^{\mathrm{p}}$ and the product of the mean particle number density, the mean

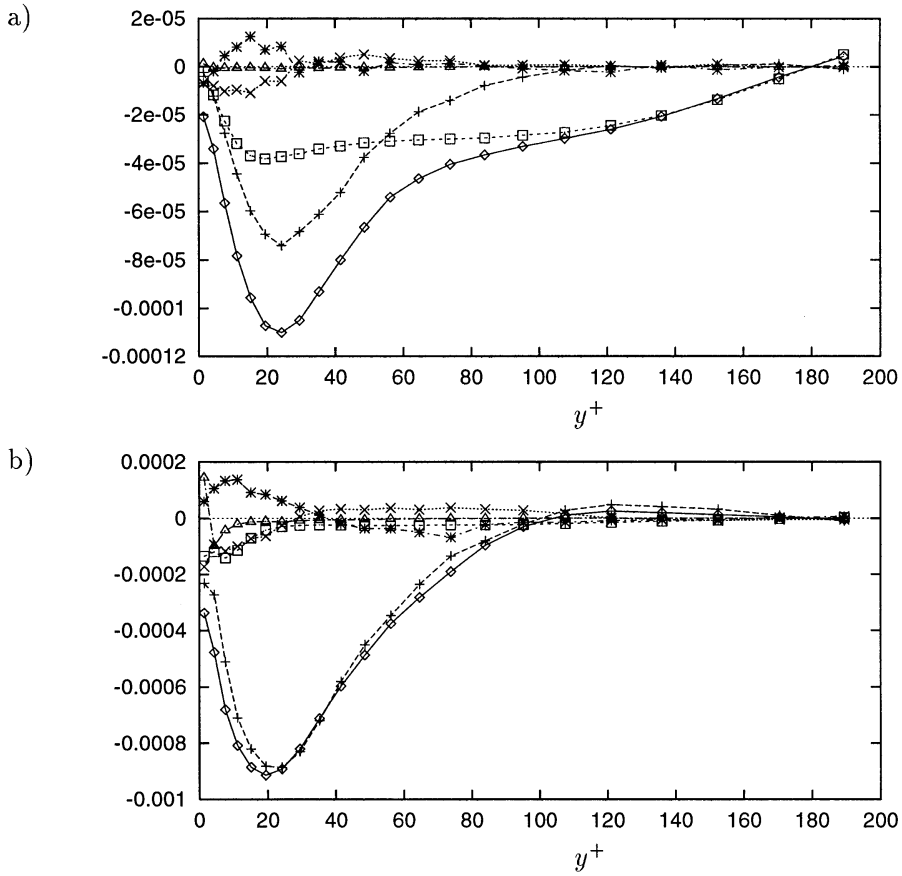

Fig. 8. Contributions to F_y^+: (a) 70 μm copper particles; (b) 50 μm glass particles. -◇-, F_y^+; - + -, $N^+ B^+ (V^{+p} - V^{+fp})$; - -□- -, $N^+ < \beta^+ (v^{+p} - v^{+f}) >^p$; - -x- -, $B^+ < n^+ (v^{+p} - v^{+f}) >^p$; - -△- -, $(V^{+p} - V^{+fp}) < n^+ \beta^+ >^p$; - -*- -, $< n^+ \beta^+ (v^{+p} - v^{+f}) >^p$.

drag coefficient and the mean relative velocity, $N^+ B^+ (V^{+p} - V^{+fp})$. In the case of 50 μm glass particles, also the correlation term, $N^+ < \beta^+ (v^{+p} - v^{+f}) >^p$, may possibly be neglected. This difference between these two cases could be due to the difference in the particle Reynolds number, shown in Fig. 9. The mean particle Reynolds number can be found roughly of order of 10 in the case of 70 μm copper particles and of order of 1 for 50 μm glass particles. The low mean particle Reynolds number made the fluctuations of β^+ negligible and reduced the contribution from $N^+ < \beta^+ (v^{+p} - v^{+f}) >^p$ to mean drag force. It is worth mentioning that the mean force due to the correlation between the fluctuating number density and the fluctuating velocity, $B^+ < n^+ (v^{+p} - v^{+f}) >^p$, and the third-order correlation, $< n^+ \beta^+ (v^{+p} - v^{+f}) >^p$, had non-zero values in the vicinity of the walls. However, at least in the cases studied here, they were found to be of the same order of magnitude with different signs and almost canceled each other.

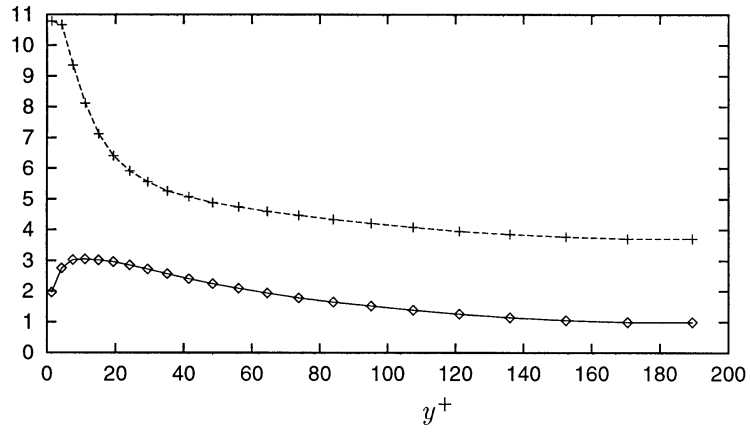

Fig. 9. Mean particle Reynolds number, $Re_p = < |\mathbf{u}^{+p} - \mathbf{u}^{+f}| d^+ >^p$. -◇-, 50 μm glass particles; - + -, 70 μm copper particles.

The terms in the averaged momentum equation in x-direction can be interpreted similarly to the y-direction equation. According to the simulation data, Fig. 10, the mean convection term, $N^+ V^{+p} \mathrm{d}U^{+p}/\mathrm{d}y^+$, the second term, $- < n^+ u^{+p} >^p \mathrm{d}U^{+p}/\mathrm{d}y^+$, and the third term, $-\mathrm{d}/\mathrm{d}y^+ \; V^{+p} < n^+ u^{+p} >^p$, were negligible in comparison to the mean drag force. The averaged drag force, F_x^+, was balanced by the sum of the transport of the streamwise particle momentum due to the wall-normal velocity fluctuation, $-\mathrm{d}/\mathrm{d}y^+ N^+ < u^{+p} v^{+p} >^p$ and the averaged gravitational force, $N^+ g^+$, see also Fig. 11.

The averaged streamwise drag force can similarly be decomposed to

$$\begin{aligned} F_x^+ &= < \tilde{n}^+ \tilde{\beta}^+ \left(\tilde{u}^{+p} - \tilde{u}^{+f} \right) >^p \\ &= N^+ B^+ \left(U^{+p} - U^{+fp} \right) + N^+ < \beta^+ \left(u^{+p} - u^{+f} \right) >^p \\ &\quad + B^+ < n^+ \left(u^{+p} - u^{+f} \right) >^p + \left(U^{+p} - U^{+fp} \right) < n^+ \beta^+ >^p \\ &\quad + < n^+ \beta^+ \left(u^{+p} - u^{+f} \right) >^p . \end{aligned} \tag{21}$$

Fig. 12 shows the contributions from the above terms to the total averaged drag force. It is found that the averaged streamwise drag force, F_x^+, can well be approximated by

$$F_x^+ = N^+ B^+ \left(U^{+p} - U^{+fp} \right). \tag{22}$$

4. Summary and conclusion

As a continuation from the previous study by the authors (Fukagata et al., 1997), motions of 70 μm copper particles and 50 μm glass particles in a turbulent channel flow at $Re_\tau = 180$ were simulated using large eddy simulation and Lagrangian particle tracking methodology. The goal of this study is to provide detailed information on various correlations which would be necessary for modeling of particulate turbulent flows.

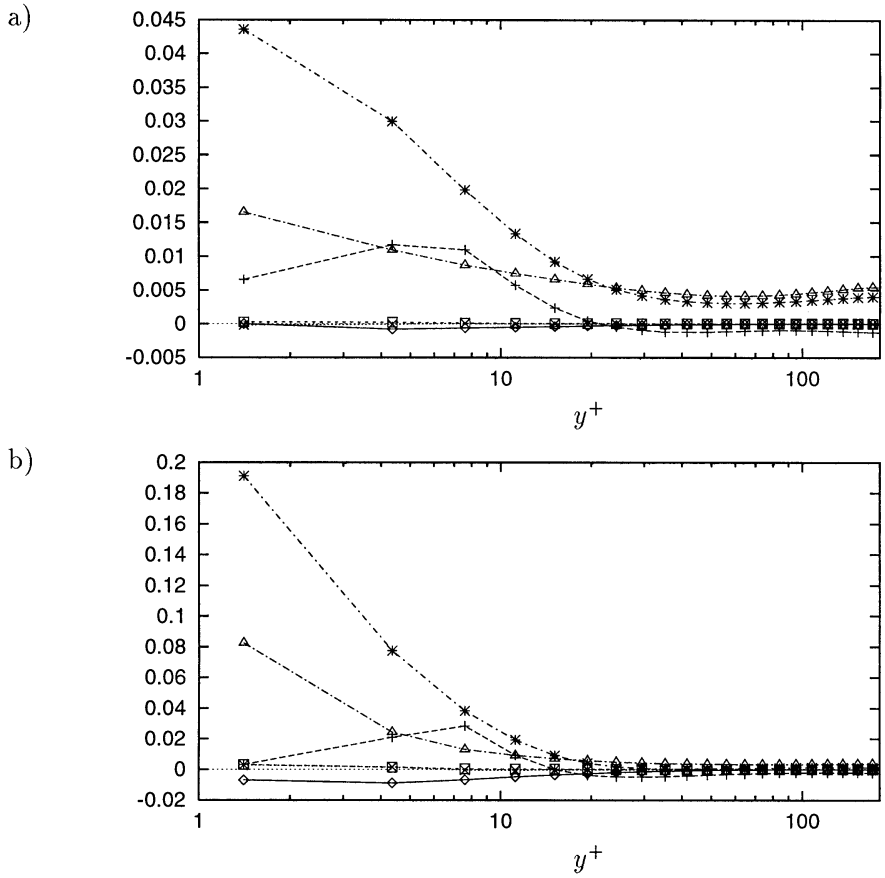

Fig. 10. Different terms in x-direction of particle momentum eqn [19]. (a) 70 μm copper particles; (b) 50 μm glass particles. -◇-, $N^+ V^{+p} \frac{dU^{+p}}{dy^+}$; -+-, $-\frac{d}{dy^+} N^+ < u^{+p} v^{+p} >^p$; - -□- -, $- < n^+ v^{+p} >^p \frac{dU^{+p}}{dy^+}$; - -x- -, $-\frac{d}{dy^+} V^{+p} < n^+ u^{+p} >^p$; - -△- -, $N^+ g^+$; - -*- -, F_x^+.

The simulation data were used for investigation of the force balances in Eulerian equation of motion for particles. The wall-normal mean drag force on particles was found to be balanced by the transport of wall-normal particle momentum due to turbulent fluctuations. The mean drag force in the wall-normal direction can be approximated by a sum of the product of the mean particle density, the mean friction coefficient and mean relative velocity in wall-normal direction, and the product of the mean particle density and correlation between the fluctuating drag coefficient and fluctuating relative velocity. Furthermore, in the case where the particle Reynolds number is of the order of unity the correlation term can also be neglected.

The streamwise mean drag force was found to be balanced by the transport of streamwise velocity due to turbulence and the gravitational forces. This component of the mean drag force can be approximated by the product of the mean particle density, the mean friction coefficient and streamwise mean velocity difference.

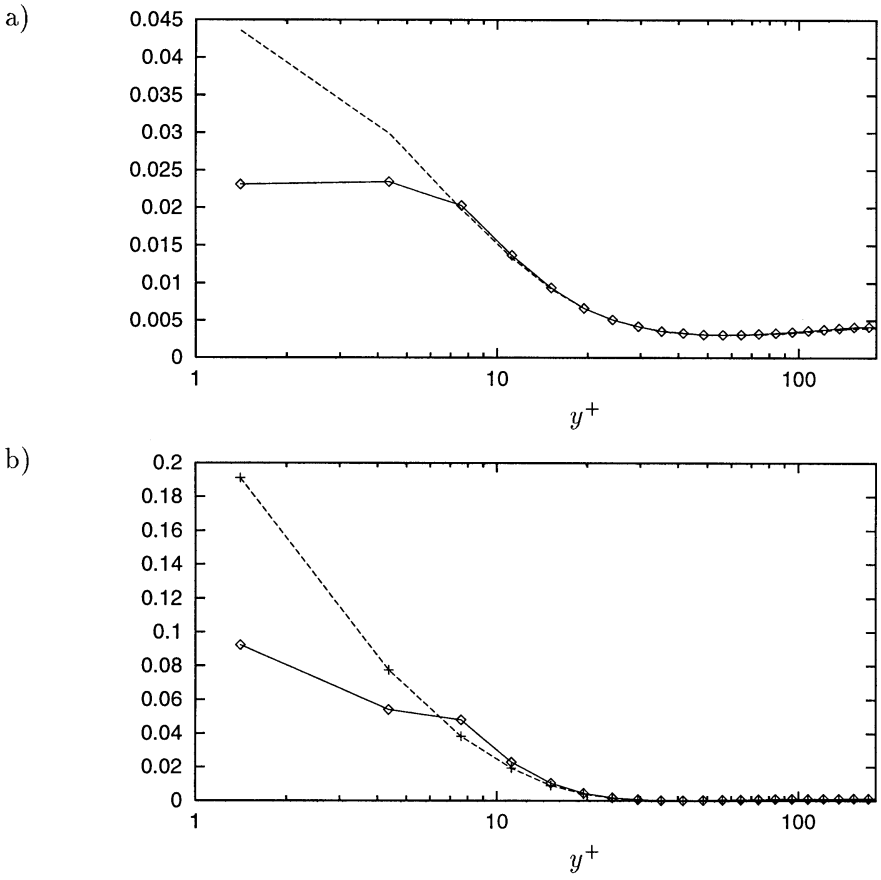

Fig. 11. Particle force balance in x-direction: (a) 70 μm copper particles; (b) 50 μm glass particles. -◇-, $-\frac{\mathrm{d}}{\mathrm{d}y^+} N^+ < u^{+\mathrm{p}} v^{+\mathrm{p}} >^{\mathrm{p}} + N^+ g^+$; - + -, F_x^+.

The simplified versions of averaged momentum equations for particle phase will read

$$\begin{cases} 0 = -\dfrac{\mathrm{d}}{\mathrm{d}y^+} N^+ < u^{+\mathrm{p}} v^{+\mathrm{p}} >^{\mathrm{p}} - N^+ B^+ \left(U^{+\mathrm{p}} - U^{+\mathrm{fp}} \right) + N^+ g^+ \\ 0 = -\dfrac{\mathrm{d}}{\mathrm{d}y^+} N^+ < v^{+\mathrm{p}} v^{+\mathrm{p}} >^{\mathrm{p}} - N^+ B^+ \left(V^{+\mathrm{p}} - V^{+\mathrm{fp}} \right) - N^+ < \beta^+ \left(v^{+\mathrm{p}} - v^{+\mathrm{f}} \right) >^{\mathrm{p}} \end{cases} . \tag{23}$$

And for low mean particle Reynolds number, one finds

$$\begin{cases} 0 = -\dfrac{\mathrm{d}}{\mathrm{d}y^+} N^+ < u^{+\mathrm{p}} v^{+\mathrm{p}} >^{\mathrm{p}} - N^+ B^+ \left(U^{+\mathrm{p}} - U^{+\mathrm{fp}} \right) + N^+ g^+ \\ 0 = -\dfrac{\mathrm{d}}{\mathrm{d}y^+} N^+ < v^{+\mathrm{p}} v^{+\mathrm{p}} >^{\mathrm{p}} - N^+ B^+ \left(V^{+\mathrm{p}} - V^{+\mathrm{fp}} \right) \end{cases} . \tag{24}$$

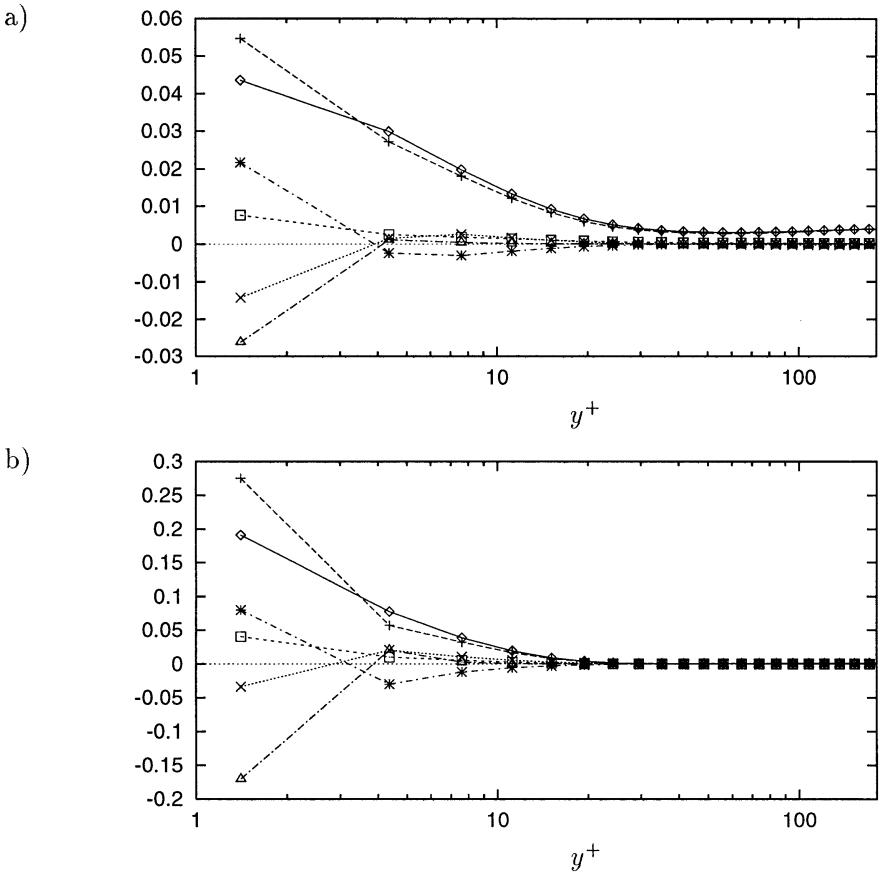

Fig. 12. Contributions to F_x^+: (a) 70 μm copper particles; (b) 50 μm glass particles. -◇-, F_x^+; - + -, $N^+B^+(U^{+p}-U^{+fp})$; - -□- -, $N^+<\beta^+(u^{+p}-u^{+f})>^p$; - -x- -, $B^+<n^+(u^{+p}-u^{+f})>^p$; - -△- -, $(U^{+p}-U^{+fp})<n^+\beta^+>^p$; - -*- -, $<n^+\beta^+(u^{+p}-u^{+f})>^p$.

References

Bolio, E.J., Sinclair, J.L., 1995. Gas turbulence modulation in the pneumatic conveying massive particles in vertical tubes. International Journal of Multiphase Flow 21, 985–1001.

Cao, J., Ahmadi, G., 1995. Gas–particle two-phase turbulent flow in a vertical duct. International Journal of Multiphase Flow 21, 1203–1228.

Chen, C.P., Wood, P.E., 1985. A turbulent closure model for dilute gas–particle flows. Canadian Journal of Chemical Engineering 63, 349–360.

Clift, R., Grace, J.R., Weber, M.E., 1978. Bubbles Drops and Particles. Academic Press, New York.

Fukagata, K., Zahrai, S., Bark, F.H., 1997. Large eddy simulation of particle motion in a turbulent channel flow, Proceedings of 1997 ASME Fluids Engineering Division Summer Meeting. FEDSM97-3591, ASME.

Kulick, J.D., Fessler, J.R., Eaton, J.K., 1994. Particle response and turbulence modification in fully developed channel flow. Journal of Fluid Mechanics 277, 109–134.

Kraichnan, R.H., 1965. Lagrangian-history closure approximation for turbulence. Physics of Fluids 8, 575–598.

Maxey, M.R., Riley, J.J., 1983. Equation of motion for a small rigid sphere in a nonuniform flow. Physics of Fluids 26, 883–889.

Mei, R., 1992. An approximate expression for the shear lift force on a spherical particle at finite Reynolds number. International Journal of Multiphase Flow 18, 145–147.

Monin, A.S., Yaglom, A.M., 1971. Statistical Fluid Mechanics: Mechanics of Turbulence, Vol. 1. MIT Press, Cambridge, MA.
Reeks, M.W., 1991. On a kinetic equation for the transport of particles in turbulent flows. Physics of Fluids A 3, 446–456.
Reeks, M.W., 1992. On the continuum equations for dispersed particles in nonuniform flows. Physics of Fluids A 4, 1290–1303.
Reeks, M.W., 1993. On the constitutive relations for dispersed particles in nonuniform flows. I. Dispersion in a simple shear flow. Physics of Fluids A 5, 750–761.
Rouson, D.W.I., Eaton, J.K. 1994. Direct numerical simulation of particles interacting with a turbulent channel flow. Proceedings of the 7th Workshop on Two-phase Flow Predictions. Sommerfeld M. (Ed.), Erlangen, Germany. .
Saffman, P.G., 1965. The lift on a small sphere in a slow shear flow. Journal of Fluid Mechanics 22, 385–400.
Swailes, D.C., Reeks, M.W., 1994. Particle deposition from a turbulent flow. I. A steady-state model for high inertia particles. Physics of Fluids 6, 3392–3403.
Tsuji, Y., Morikawa, Y., Shiomi, H., 1984. LDV measurement of an air–solid two-phase flow in a vertical pipe. Journal of Fluid Mechanics 139, 417–434.
Wang, Q., Squires, K.D., 1996a. Large eddy simulation of particle-laden turbulent channel flow. Physics of Fluids 8, 1207–1223.
Wang, Q., Squires, K.D., 1996b. Large eddy simulation of particle deposition in a vertical turbulent channel flow. International Journal of Multiphase Flow 22, 667–683.
Zahrai, S., Bark, F.H., Karlsson, R.I., 1995. On anisotropic subgrid modeling. European Journal of Mechanics, B/Fluids 14, 459–486.